ARTICLE

TECHNOLOGY

A scale-up nanoporous membrane centrifuge for reverse osmosis desalination without fouling

Qingsong Tu[1], Tiange Li[1], Ao Deng[2], Kevin Zhu[3], Yifei Liu[4] & Shaofan Li[1]

A scale-up nanoporous membrane centrifuge is designed and modeled. It can be used for nanoscale scale separation including reverse osmosis desalination. There are micron-size pores on the wall of the centrifuge and nanoscale pores on local graphene membrane patches that cover the micron-size pores. In this work, we derived the critical angular velocity required to counter-balance osmosis force, so that the reverse-osmosis (RO) desalination process can proceed. To validate this result, we conducted a large scale (four million atoms) full atom molecular dynamics (MD) simulation to examine the critical angular velocity required for reverse osmosis at nanoscale. It is shown that the analytical results derived based on fluid mechanics and the simulation results observed in MD simulation are consistent and well matched. The main advantage of such nanomaterial based centrifuge is its intrinsic anti-fouling ability to clear N_a^+ and Cl^- ions accumulated at the vicinity of the pores due to the Coriolis effect. Analyses have been conducted to study the relation between osmotic pressure, centrifugal pressure, and water permeability.

***Keywords*: Desalination; Fouling; Graphene; Molecular Dynamics; Nanoporous Membrane; Reverse Osmosis.**

1. INNOVATION

The nanomaterial-based reverse osmosis (RO) desalination technology has shown great potential in providing an energy efficient means to solve the global water resource problem. On the other hand, the current nanomaterial-based RO desalination technology faces two major challenges: (1) Fouling problem and (2) scale-up problem. There are three innovations of this work: (1) We have discovered that the rotating nanoporous membrane centrifuge has no ion concetration polarization, which is a clear indication and explanation of why the proposed nanoporous membrane centrifuge has no fouling; (2) We have derived the critical angular velocity of the nanoporous membrane centrifuge based on the Navier-Stokes equation, and have compared it with the computed critical angular velocity based on molecular dynamics, and (3) We have proposed a possible scaling-up strategy to fabricate such nanoporous membrane centrifuge in macroscale.

2. INTRODUCTION

Fresh clean water is essential to human health and for the survival of human society and civilization. The world is facing daunting challenges in meeting rising demands of clean fresh water as the available natural water resources are limited and decreasing due to climate change, industrial globalization, and human population growth. Nanomaterials have a number of key physicochemical properties that make them particularly attractive as separation media for water purification. Over the past decade, exciting progress has been made on research and development of carbon nanotube and graphene based nanoscale membranes for reverse osmosis desalination[1–8]. However, there are some daunting challenges to turn nanomaterials based membrane technology into practical use. (a) Fouling problem: Most graphene-based membranes have serious blockage problems due to interactions between cations and aromatic rings in CNTs or graphene membranes[9,10]. (b) Energy consumption problem: In classic RO technology, the osmotic pressure is balanced by applying external pressure directly onto the salt water, which requires ultrahigh pressure and hence high energy consumption[11]. Currently, all practical laboratory graphene membrane devices still have not shown high energy efficiency as promised. (c) Scale-up problem: How to synthesize or manufacture a scale-up graphene membrane that can actually make salt water into fresh water at large scale is still not attainable at the moment[12].

In Ref. 13, we proposed an idea of nanoscale graphene-membrane centrifuge to fundamentally resolve these issues. However, that idea was not adequately elaborated, so that it can directly link to engineering desalination applications. In this paper, we shall focus on how to resolve the two fundamental issues in the scaling-up effort: (1) How to scale-up the nanoscale graphene membrane centrifuge reported in Ref. 13 to fabricate a macroscale nanoporous membrane centrifuge, and (2) why and how the proposed nanoporous membrane centrifuge is free of fouling.

To scale-up the nanoscale graphene-membrane centrifuge into a macroscale membrane desalination machine, there are two tasks to be undertaken: (a) How to make a macroscale nanoporous membrane centrifuge, and (b) What is the angular velocity needed for a macroscale nanoporous membrane centrifuge to perform practical desalination operation?

[1]University of California, Berkeley, CA 94720, USA. [2]Beihang University, 100191 Beijing, China. [3]Amador Valley High School, Pleasanton, CA 94566, USA. [4]WHBC of Wuhan Foreign Languages School, Wuhan, China, 430022. Correspondence should be addressed to: S.L. (shaofan@berkeley.edu).

Received 8 November 2017; accepted 2 March 2018; published online 29 March 2018; doi:10.1142/S2339547818500024

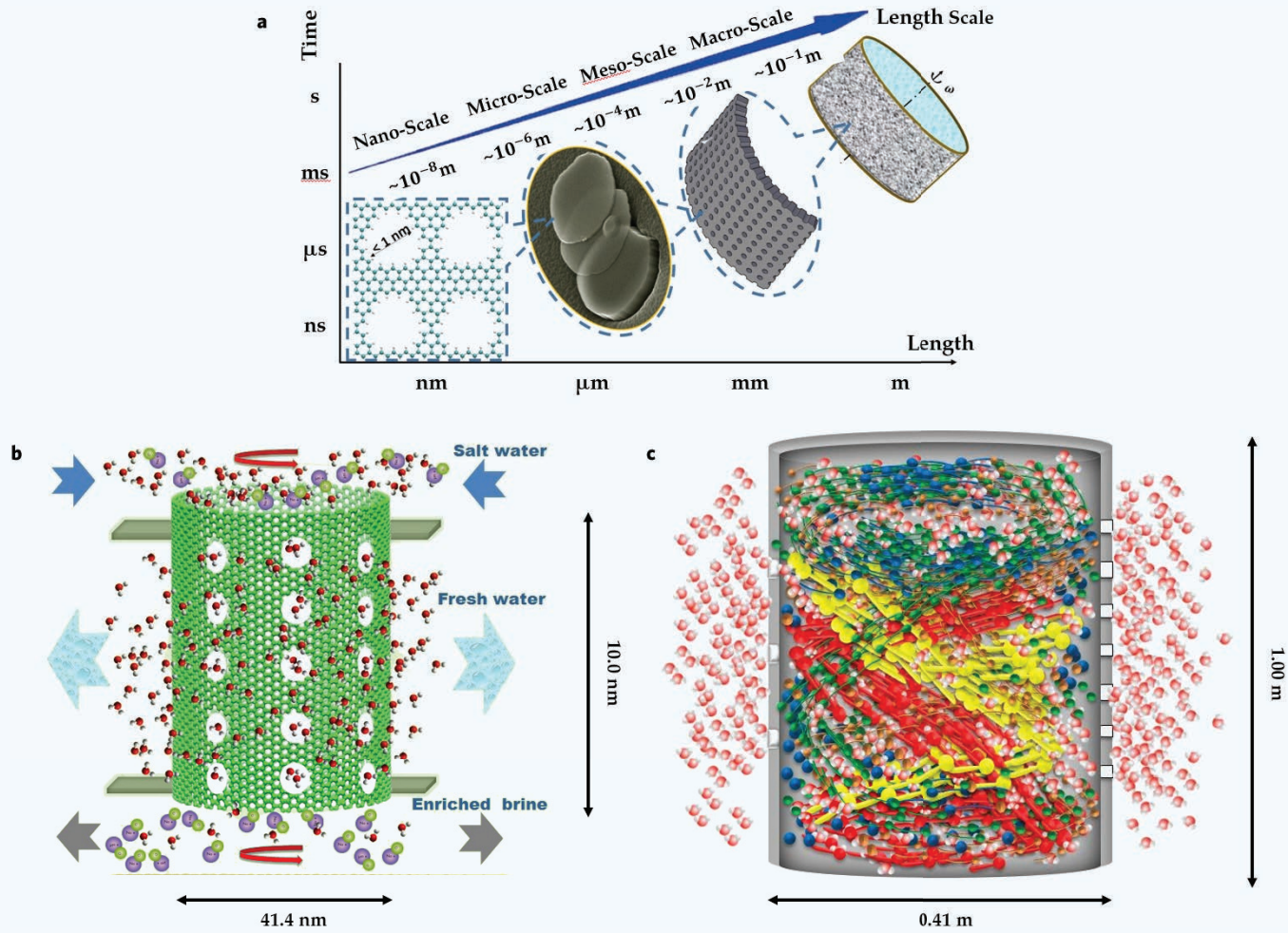

Figure 1 Schematic illustration of the concept on how to scale up nanoscale graphene centrifuge to a macroscale graphene centrifuge that has a multiscale pore structure: (**a**) multiscale centrifuge structure, (**b**) nanoscale graphene centrifuge, and (**c**) macroscale centrifuge.

To answer the first question, in **Fig. 1**, we propose a concept of a multiscale porous membrane centrifuge that has a multiscale pore structure. As shown in **Fig. 1a**, the macroscale centrifuge can be made by conventional metallic or polymatric materials that can provide strength support for the structure. We can then create many small holes with diameters at micron scale by using the laser pulse technology[14] on the wall of a macroscale centrifuge. On the opening of each macroscale pore, we can cover it with a layer of porous nanomaterial membrane, which can be a single layer of porous graphene with many microscale holes with diameters at nanometer or sub-nanometer scale (see **Fig. 1a**), or multilayers of graphene, graphene oxide (GO) or MoS_2 etc. These nanoscale pores may be created by using ion bombardment method[15] or e-beam lithography[16], so that it provides a fine scale membrane that can separate fresh water molecules from Na^+ and Cl^- ions, if we carefully select the size of nanoscale pore. As described in literature e.g. Ref. 17, hydrated Na^+ and Cl^- are surrounded by 4 to 6 water hydration shells, which have an effective diameter around 2.7 nm, if the size of nanopores are controlled around 1 nm, filtration of fresh water will be possible. By doing so, the metallic or polymeric wall of the macroscale centrifuge can provide strength of the desalination machine, while the locally embedded nanoporous membrane will provide the function of water filtration. We will answer the second question in the later sections.

Because of the limitation of computational resource, we only employ molecular dynamics to investigate the working principle or the desalination mechanism of the nanoporous graphene membrane centrifuge as illustrated in **Fig. 1b**. In practical design and fabrication, one may make multiple level pores of different length scales on different sheets or thin foils, layer by layer, such that it makes the multiscale porous centrifuge equivalent to the nanoporous membrane centrifuge shown in **Fig. 1c**, in principle.

3. RESULTS

A sequence of snapshots of MD simulation results are displayed in **Fig. 2**. One may find that water molecules flow out from the pores on the rotating centrifuge wall continuously while Na^+ and Cl^- ions are blocked inside.

3.1. Water density distribution

Water density distribution inside the centrifuge provides key information on the overall water molecule motions during the desalination process. In **Fig. 3a**, we plot the water density distribution along radial directions for different angular velocities. For the case of the angular velocity $\omega = 34.91$ *rad/ns*, we show the water density distribution in a half of longitudinal section of the graphene centrifuge in **Fig. 3b**.

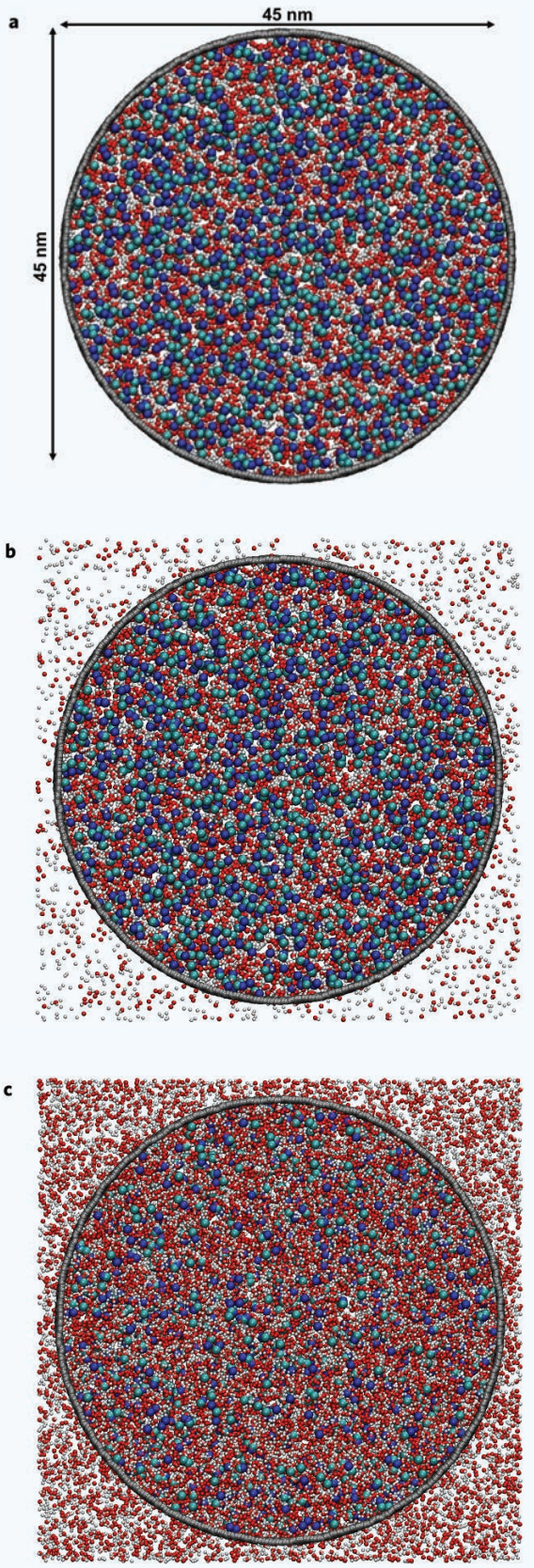

Figure 2 Time sequence of MD simulation of water filtration in a nanoporous graphene membrane centrifuge with four million water molecules. Section views: (**a**) 0.0 ns, (**b**) 1.5 ns, and (**c**) 3.0 ns.

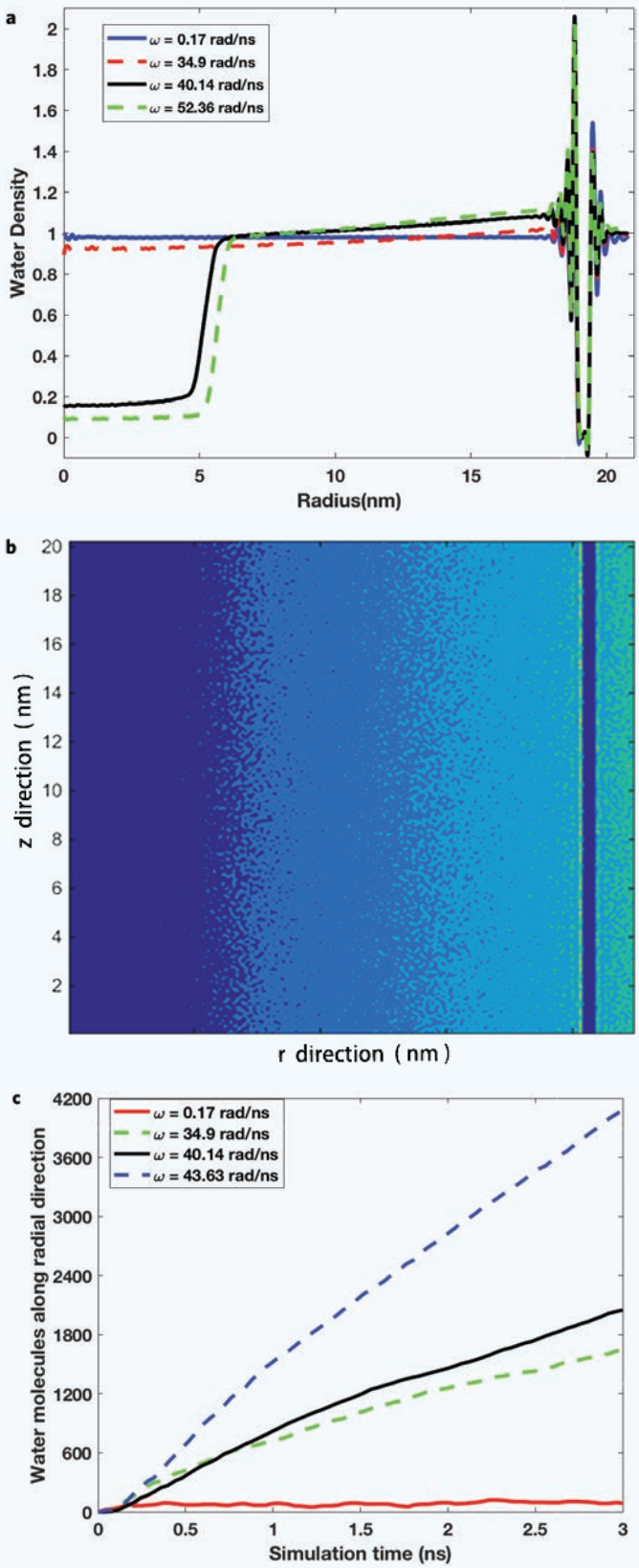

Figure 3 Water density distribution inside and outside of the graphene centrifuge: (**a**) water density distribution in radial direction, (**b**) water density distribution in physical space (a longitudinal section of simulation box), and (**c**) fresh water filtration volume.

One can see that there are some oscillatory changes in water density profile near and across the graphene wall (around 2 nm region). These oscillating changes reflect the process of water molecule accumulation to the graphene wall (driven by the centrifugal force), filtration through the graphene wall, and diffusion in the ambient space after they are out of the centrifuge. For other areas, the water density is almost uniform, except at the 5 nm mark, there is a sudden jump, which indicates the formation of a vortex in the center region of the centrifuge. This phenomenon only happens under certain angular velocities, which itself is an interesting topic at nanoscale, and it will be discussed in detail in a subsequent paper.

We plot the number of water molecules filtered through the centrifuge under different angular velocities in **Fig. 3c**. One can find that the number of the fresh water molecules filtered through increases as the angular velocity of the centrifuge increases. However, this has a limit. If the angular velocity of the centrifuge reaches to a certain level, the centrifuge pressure will be large enough to break the hydration shell of the ions, so that ions will pass out through the pores on the graphene wall. This phenomenon was discussed in Ref. 13.

3.2. Tangential velocity field

As mentioned above, one of the main advantages of the graphene membrane centrifuge is its self-assisted clean mechanism to keep clear of the entrance of pores on the membrane wall. This is because the rotating motion of the graphene centrifuge not only generates centrifugal force but also the Coriolis force as well, which generates a tangential force field along the membrane wall of the centrifuge to keep heavy atoms moving all the time without staying in the same location. To quantify this self-assistant anti-fouling effect of the model, we measured the relative tangential velocity of the flow field adjacent to the graphene wall, i.e. $\mathbf{v}_r^t = \mathbf{v}_{atom}^t - \mathbf{v}_w^t$, where $v_w^t = R\omega$. In **Fig. 4a**, we plot the time history of both average relative tangential velocity of water molecules and ions. Because of the difference in mass weight, one may find that the magnitude of the tangential velocity of ions is almost six times larger than that of water molecules, which makes the ions moving along the tangential direction of the membrane wall without staying near the same location. In addition to have small mass weight, water molecules may penetrate through the porous graphene wall, which reduces their tangential force interaction with the graphene wall, and this may be another reason why they have less tangential velocity.

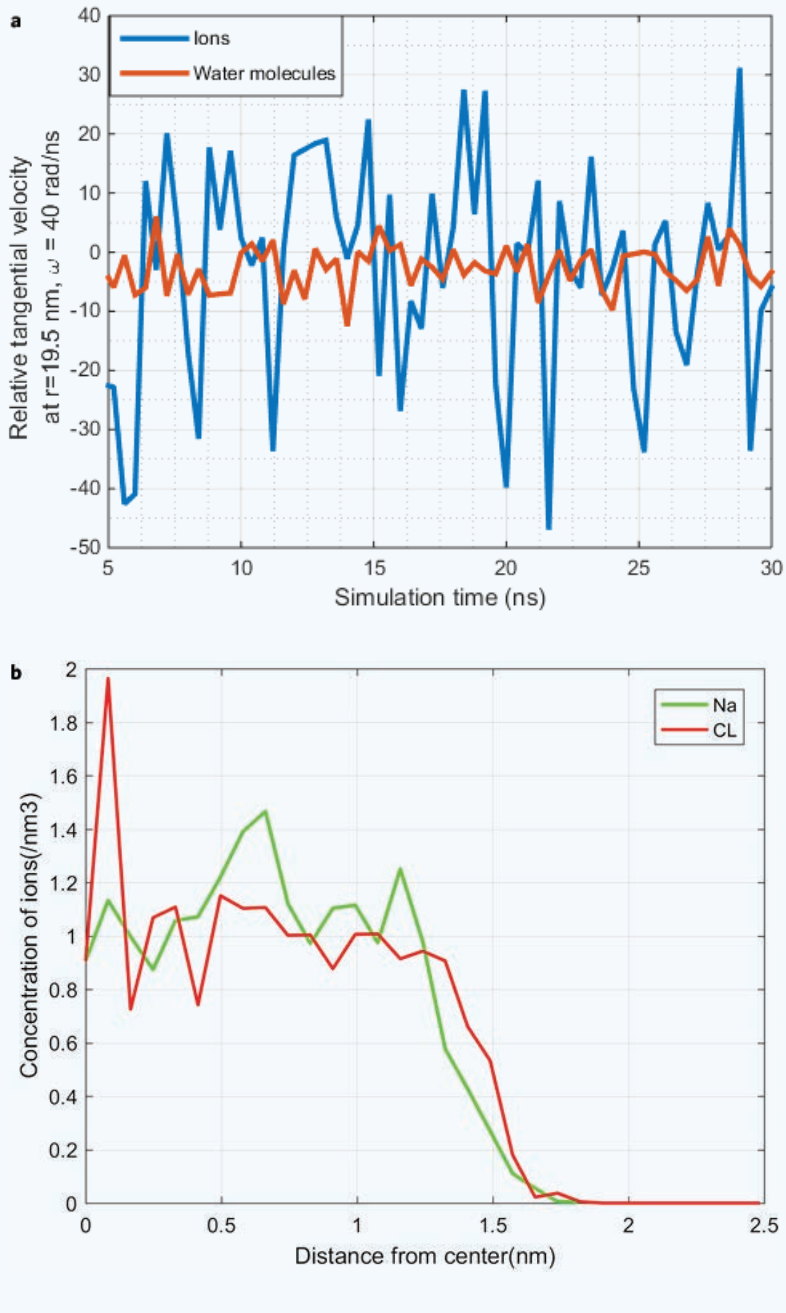

Figure 4 (**a**) The average relative tangential velocity history of the water molecule and ions near the graphene wall and (**b**) ion density concentration distribution along the radial direction of the nano-porous membrane centrifuge.

To verify this observation, in a preliminary study, we studied the ion density distribution along the radial direction of the porous membrane centrifuge of a different size (2 nm in radius), and we plot the ion density distribution in **Fig. 4b**. **Figure 4b** shows that there is almost no ion concentration near the membrane wall. This is the main discovery of the reported research, which is a direct proof or evidence that the proposed nanoporous membrane centrifuge is fouling-free.

3.3. Centrifugal pressure, total pressure and angular velocity

The pressure generated by the centrifugal force is directly related to the angular velocity of the graphene membrane centrifuge. At macroscale, this relation is explicitly expressed in Equations (21) and (23). Based on Equation (27), the critical angular velocity needed to balance osmotic pressure for a graphene centrifuge of radius $R = 20.715\ nm$ is about $\omega_{cr} \approx 3.6\ rad/ns$. In order to calibrate the critical angular velocity obtained by using macroscale fluid mechanics, we compare it with that obtained from MD simulations. And we plotted the relation between total pressure and the angular velocity in **Fig. 5a**.

In equilibrium statistical molecular dynamics, pressure is a statistical variable, and it is calculated by using the Virial theorem, which requires the interaction forces and velocities of every atom in the entire molecule ensemble. However, the graphene membrane centrifuge is a non-equilibrium system. In order to calculate the net pressure onto the graphene wall, we adopt an elementary approach. The centrifugal pressure is defined as the net centrifugal force acting on the graphene wall divided by the wall area, and the centrifugal force is computed according to Equation (28).

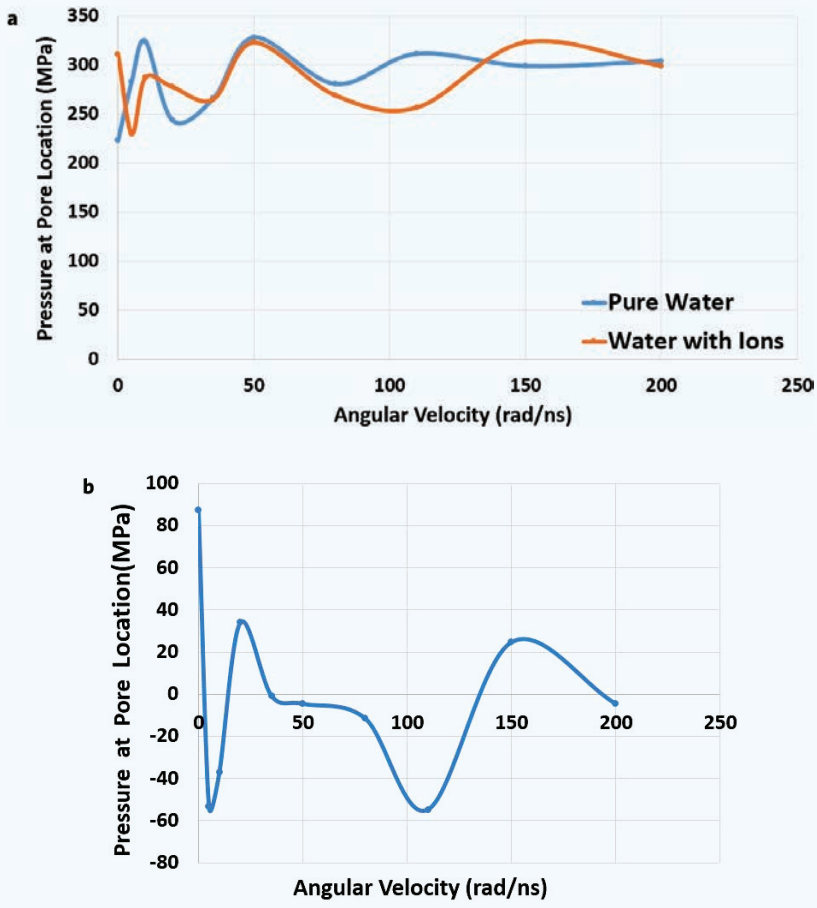

Figure 5 (**a**) The relationship between angular velocity and total pressure at the pore location and (**b**) osmotic pressure at different angular velocities.

The calculated pressure-angular velocity relation is shown in **Fig. 5a**. Note that when $\Delta P = 0 \rightarrow p_{\omega} = p_{cr} = \Pi \approx 27.8\ Bar$ (see Section 5), which is the threshold value for water filtration to proceed. Based on fluid mechanics prediction, only when the centrifugal pressure is higher than this value will water molecules move out of the centrifuge. After this point, fresh water flow rate increases quadratically (solid line) with the increase of angular velocity. The MD simulation results (dots) agree with the prediction based on fluid mechanics.

We also studied the relationship between angular velocity and the total pressure of water at the pore locations. To calculate the pressure, we developed two models using Gromacs[18]. Both of the models use a giant-size CNT serving as graphene membrane cylinder with chirality number (20,40) and length 6.8 nm. There are 12 pores created on the graphene wall with pore diameter $d = 0.78\ nm$. We solvated both CNTs into water boxes with dimensions of $6.01 \times 6.06 \times 7.98\ nm$. The only difference between these two models is that we added Na^+ and Cl^- ions in one of the models while we replaced those ions with water molecules in the other model. As for the model with ions, we added Na^+ and Cl^- ions with a total number of 48 pairs, which corresponds to the concentration of salt ions in seawater (35 g/L). In addition, there are a total of 7608 water molecules in this model, while the other model has a total of 7656 water molecules without any ions.

As indicated in Section 4 the total pressure of water at a pore location is the combined result of different kinds of pressure. Under the assumption that the positive direction of pressure is the direction towards the outside of the CNT, in terms of the model with ions (we label it "Model A" in the following discussions), total pressure should be equal to the osmotic pressure subtracted from the centrifugal pressure. For the model without ions (labeled as "Model B"), total pressure is actually equal to the centrifugal pressure itself, because of the lack of the osmosis phenomenon. So if we subtract the pressure outcome of these two models, the result should be the value of osmotic pressure at the pore location.

Figure 5a shows the total pressure at the pore location of the two models. This result was obtained by counting the number of water molecules at the pore location and dividing the total force of these water molecules by the area of pore. In **Fig. 5b**, we display the value of osmotic pressure, computed as the pressure difference between Models A and B, for different angular velocities. From this figure, we can tell that there is a sudden change in pressure at a certain angular velocity, which may be caused by the small number of ions passing through the pores. However for larger angular velocities, the osmotic pressure stays stable and does not change much with angular velocity, which shows coherence with our theoretical analysis that indicates that osmotic pressure should be constant. Moreover, we calculate the average value of osmotic pressure at different angular velocities and the result is 2.1143 *MPa*, while the theoretical value of osmotic pressure is 2.78 *MPa*, which is reasonably close to our simulation result[19].

However, as described later, there are still some differences between the MD simulation results and the analysis based on macroscale fluid mechanics. This can be attributed to the difference between macroscopic scale phenomena and microcosmic molecular motions. Macroscopic phenomena are the statistical reflections of massive numbers of molecules. Due to the limitation of MD simulations including the size of the MD models and time duration of the simulation, MD simulation results presented here may be able to capture fine scale details of a macroscale event, because the number of water molecules taking part in MD simulation is much smaller compared to that of water molecules participating in a macroscale desalination process. For example, the CNT centrifuge model built in MD simulation has a length of 10 nanometers, and the diameter of pores on the graphene membrane wall is only 0.78 nanometer. Because the pore size is so small, there are only approximately 30 water molecules within cut-off distance of a given pore location. Apparently, this amount of molecules is much smaller than that needed to describe an actual macroscale fluid flow event. Because of the uncertainty in the movement of a single molecule, when the amount of molecules is too small, these molecules altogether can hardly reproduce the macroscopic phenomenon. Hence these are the sources of differences between the macroscale theoretical analysis and the microscale simulation results.

Nevertheless, this does not mean that there is no relationship between our microscale results and the macroscale theory. Microscale simulation may not be able to model the entire macroscale desalination process, but does provide general understanding on macroscale desalination mechanism. Differences between macroscopic phenomena and microscale molecular simulations may come from different sources, such as numerical errors, size effects, time scale, and approximation of phenomenological theory, etc. Thus, it is reasonable to expect that MD simulation results may differ from the results obtained from macroscale fluid mechanics analysis.

3.4. Fresh water filtration rate

Figure 6a shows the fresh water flux number of the porous membrane centrifuge under different angular velocities during MD simulations. One may find that when $\omega < 5$ *rad/ns* there is almost no net filtration fresh water flux, and the fresh water flux is negative, i.e. this is the case of the inward water flow. **Figure 6b** shows the fresh water filtration rates obtained from both analytical calculation of fluid mechanics (see Equation (31)) and MD simulation result. The numerical result was obtained by counting the number of water molecules moving out from pores on the graphene wall. From **Fig. 6b**, one can see that the MD prediction of fresh water flow rate is close to that of analytical result of fluid mechanics. However, when the radius of the centrifuge is too small, the two may have big discrepancies, e.g. Ref. 19.

The fresh flow rate increases quadratically as the angular velocity increases; however, when ω becomes too big, the centrifugal pressure may break the hydration bond between the ions and water molecule, such that it will also push the ions out, or keep the ions in the pore, which will decrease the purity of desalination. Therefore, there is an optimal angular velocity for reverse osmosis, and in this simulation, it is 40 *rad/ns* (see **Fig. 6a**), which was used in the latter analysis.

3.5. Energy efficiency

In industry practice, there are several desalination methods, and the main focus of desalination technology is in its energy efficiency. For the nanoporous graphene centrifuge model present here, we attempt to provide a theoretical estimate for the lower bound of its energy consumption, which is calculated by the following formula,

$$\eta = \frac{\text{Energy Input}}{\text{Fresh water outcome}}, \tag{1}$$

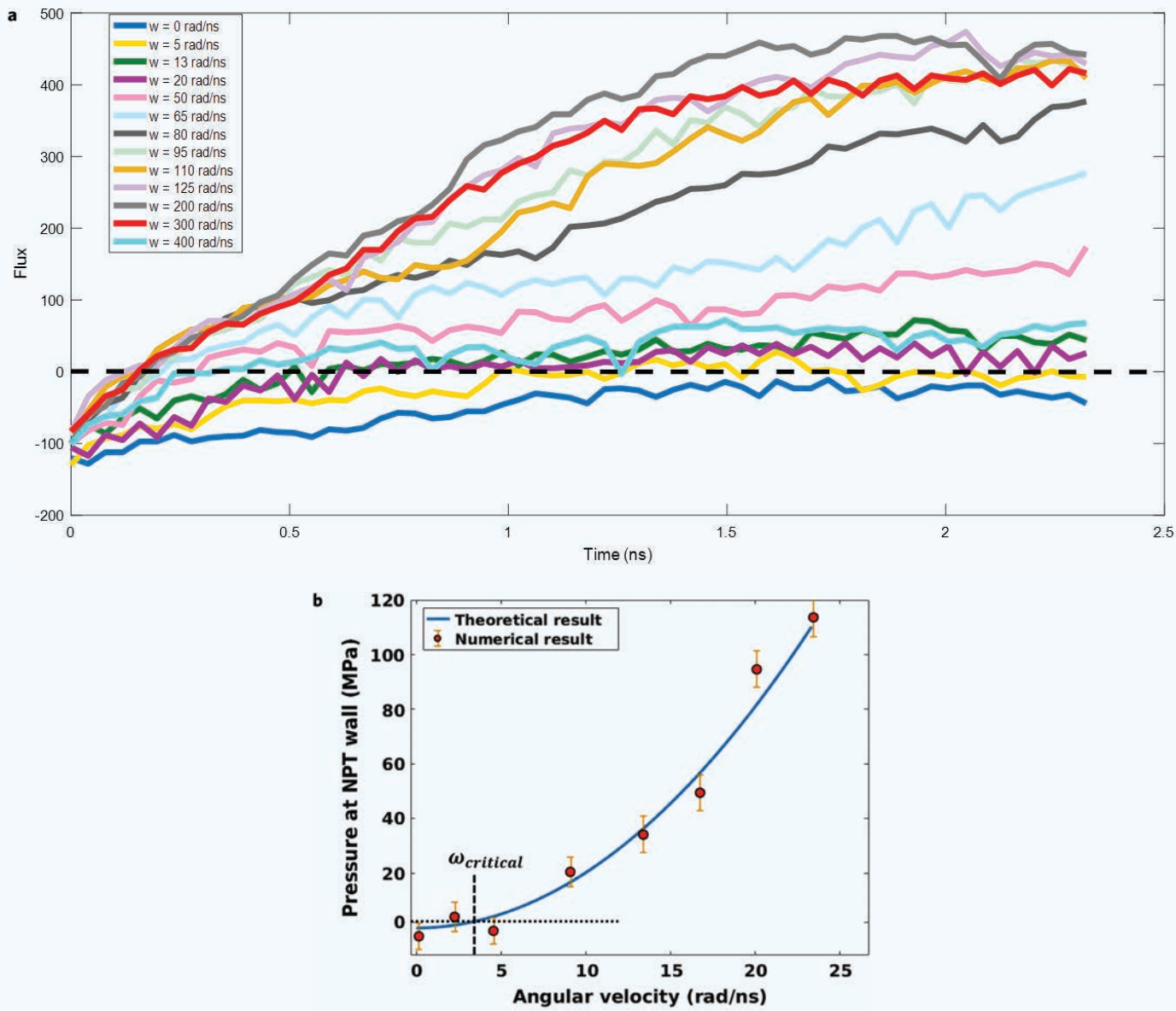

Figure 6 (**a**) Fresh water flux number of the nanoporous membrane centrifuge under different angular velocities and (**b**) comparison of the critical angular velocity obtained from that obtained from fluid mechanics calculation and that obtained from the molecular dynamics simulation. **Solid line:** The analytical result obtained from fluid mechanics, **Black dots:** the numerical result obtained from MD simulation.

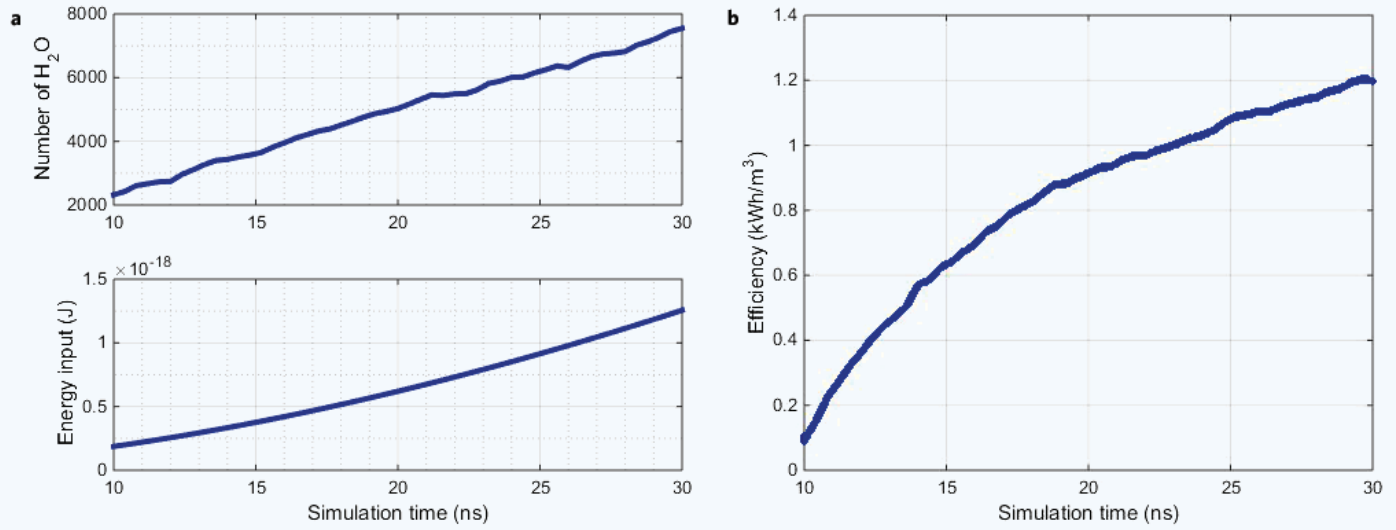

Figure 7 (**a**) The energy input and number of water molecules moving out and (**b**) computed energy efficiency.

where the *Energy Input* is defined as the change of kinetic energy when fresh water overcoming the thermodynamics free energy barrier moving out of the centrifuge (without counting overhead); and *Fresh Water Outcome* is defined as the total number of water molecules going through the filtration process in the simulation.

We have conducted a longer time simulation (30 *ns*) with an angular velocity ($\omega = 40$ *rad/ns*) as shown in **Fig. 7**. In this case, both the energy input and fresh water outcome increase linearly as a function of simulation time. The average value for energy input and number of water molecules are 4.2697×10^{-19} *J* and 1960.13, respectively. Using the following unit transform:

$$1\ J = 2.78 \times 10^{-7}\ kWh \tag{2}$$

The volume of N water molecules:

$$V_N = \frac{N \times M_{H_2O}}{\rho_{H_2O}} = 2.9N \times 10^{-29} m^3 \tag{3}$$

Therefore, the final result for efficiency during the simulation time is:

$$\eta = \frac{2.2697 \times 10^{-19} \times 2.78 \times 10^{-7}\ kWh}{2.9 \times 1960.13 \times 10^{-29} m^3} = 1.1\ kWh/m^3, \tag{4}$$

which appears at the lower end among all RO desalination methods.

4. ANALYSIS AND DISCUSSIONS

We illustrate the reverse osmosis mechanism of the proposed multi-scale centrifuge in **Fig. 8**. Without considering mass transport in axial direction, the complex molecular interaction among atoms and molecules near the pore that dictate the water filtration process may be characterized by three main macroscale forces acting on water molecules or hydrated ions: The centrifugal force, the Coriolis force, and the osmosis force. We note that the osmosis force is an entropic force, but not the Newtonian force, so that the force diagram in **Fig. 8** is a not strictly a force equilibrium diagram.

According to the transport theory in membrane, a Hagen-Poiseuille equation can be used to describe the volumetric flow rate of a single pore on the membrane:

$$Q(\varepsilon, r_p, \Delta P) = N_p \frac{\pi r_p^4 \Delta P}{8\mu_0 L_m} = \frac{\varepsilon r_p^2 A_m}{8\mu_0 L_m} \Delta P \tag{5}$$

where Q is the volumetric flow rate of water through a pore; L_m is the membrane pore length. r_p is the pore radius; μ_0 is the dynamic viscosity of water; N_p is the number of pores within an membrane area of A_m; ε is the porosity of the structure, and ΔP is the net pressure difference of the two sides of the membrane.

From the above equation, we can obtain the water flux and permeability defined as follows,

$$J_w(\varepsilon, r_p, \Delta P) = \frac{Q(\varepsilon, r_p, \Delta P)}{A_m} = \frac{\varepsilon r_p^2}{8\mu_0 L_m} \Delta P, \tag{6}$$

and

$$A(\varepsilon, r_p) = \frac{J_w(\varepsilon, r_p, \Delta P)}{\Delta P} = \frac{\varepsilon r_p^2}{8\mu_0 L_m}. \tag{7}$$

As shown in the above equations, the fresh water filtration rate depends on pressure difference across the membrane, but the permeability only depends on the geometric parameter of the membrane. To obtain an estimate, one needs to find the pressure difference ΔP, or the pressure generated by the centrifugal force p_ω.

As shown in **Fig. 8**, the small scale centrifuge is comprised of semi-permeable membranes, which separate the molecular system into two compartments: The pure water is outside the container and the salt water is inside the container. Since the porous membrane has many holes, an osmotic force will present along the radial direction pointing inward of the membrane, because of the ion concentration difference of the two compartments. Hence driven by the osmosis pressure, water molecules will diffuse into the centrifuge, if the centrifuge

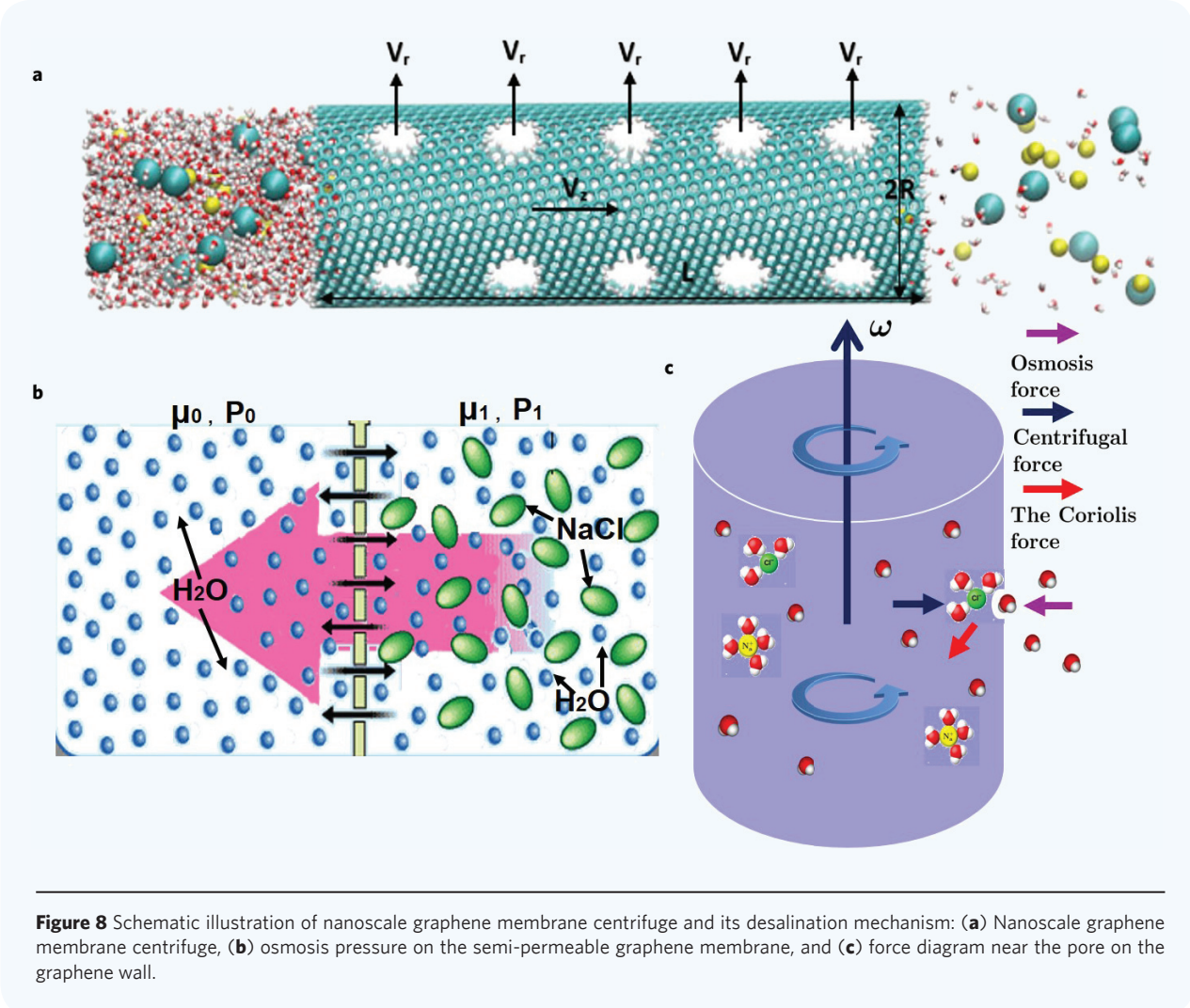

Figure 8 Schematic illustration of nanoscale graphene membrane centrifuge and its desalination mechanism: (**a**) Nanoscale graphene membrane centrifuge, (**b**) osmosis pressure on the semi-permeable graphene membrane, and (**c**) force diagram near the pore on the graphene wall.

is not rotating. However, when the centrifuge starts to rotate with an angular velocity Ω, a centrifugal force will be generated on every atom in the system pointing in the outward direction, and it increases as Ω increases.

If we set the pressure outside the container as ambient pressure P_0, then the pressure inside can be viewed as the net value of three parts:

$$P_1 = P_0 - \Pi + P_{ext} \tag{8}$$

where P_{ext} is the external pressure applied to overcome the osmotic pressure Π. Since the osmotic pressure is obviously always opposite to external pressure, we can then define the pressure difference as:

$$\Delta P = P_1 - P_0 = P_{ext} - \Pi. \tag{9}$$

The reverse osmosis process is to generate a large enough P_{ext} to ensure ΔP is greater than zero, and water molecules can separate from saltwater flowing into side of pure water. In this work, the external pressure P_{ext} is introduced by the centrifugal force.

The osmotic pressure Π is dependent on the concentrations of Na^+ and CL^- ions and internal pressure of the system, and it is essentially a thermodynamic property of the molecular system[20]. For a given molecular system, it may be calculated by using molecular dynamics.

In this work, for the purpose of environmental engineering applications, a practical formula that is used widely to estimate osmosis pressure in sea water is adopted,

$$\Pi = \frac{C}{N_a}\frac{TN_i}{M_s}, \tag{10}$$

where N_i is the number of ion pairs (Na^+ and Cl^-); C is a constant value: $C = 0.1544$, Na is the Avogadro Constant; T is temperature, in Kelvin; M_s is the mass of solvent, in kilograms. The unit of Π is in Bar.

Customarily, the external pressure P_{ext} is denoted as the pressure applied directly on saltwater by external weight; however, in the current study, P_{ext} is generated by rotation of the centrifuge. When the centrifuge rotates with an angular velocity ω, the centrifugal force will push water moving out, which is equivalent to applying a pressure P_ω near the wall of the container; this new variable will serve as the external pressure to balance osmotic pressure in the solution: $P_{ext} = P_\omega$. We now derive the expression of the pressure by treating the problem as a Newtonian circular Couette flow.

The Navier-Stokes equation in fluid mechanics may be written as follows:

$$\rho\left(\frac{\partial \mathbf{v}}{\partial t} + \mathbf{v}\cdot\left(\nabla \times \mathbf{v}\right)\right) = \nabla\cdot\sigma \tag{11}$$

where ρ is the density and σ is the stress. For Newtonian fluid with dynamic viscosity μ_0, the stress can be expressed as:

$$\sigma = -p_\omega \mathbf{I} + 2\mu_0 \dot{\boldsymbol{\varepsilon}} \tag{12}$$

where $\mathbf{I}$ is the second order unit tensor, and the components of the strain rates $\dot{\boldsymbol{\varepsilon}}$ are given as,

$$\dot{\boldsymbol{\varepsilon}}_{ij} = \frac{1}{2}\left(\frac{\partial v_i}{\partial x_j} + \frac{\partial v_j}{\partial x_i}\right) - 1/3(\nabla \cdot \mathbf{v})\delta_{ij}. \tag{13}$$

where $\mathbf{v}$ is the velocity field. Next, we first assume that both the axial velocity field and the velocity field of filtration flow is negligible in comparison with the circular flow field, which is usually at least two or three orders of magnitude bigger than the two other flow fields. Additionally, we assume that the flow field is axisymmetric, and thus, $v_r = v_z = 0$, and $v_\theta = v_\theta(r)$.

The circumference flow field can then be determined from the integration of the linear momentum equation in the θ-direction,

$$\rho\left(\frac{\partial v_\theta}{\partial t} + v_r\frac{\partial v_\theta}{\partial r} + \frac{v_\theta}{\partial r}\frac{\partial v_\theta}{\partial \theta} + v_z\frac{\partial v_\theta}{\partial z} + \frac{v_r v_\theta}{r}\right) = \frac{\partial \sigma_{r\theta}}{\partial r} + \frac{1}{r}\frac{\partial \sigma_{\theta\theta}}{\partial \theta} + \frac{\partial \sigma_{\theta z}}{\partial z} + \frac{2\sigma_{r\theta}}{r}. \tag{14}$$

For steady flows, the above equation reduces to

$$\frac{1}{r^2}\frac{d}{dr}\left(r^2\sigma_{r\theta}\right) = 0, \quad \text{with} \quad \sigma_{r\theta} = \frac{\mu}{2}\left(\frac{\partial v_\theta}{\partial r} - \frac{v_\theta}{r}\right). \tag{15}$$

When $r < R$, integrating (15) over r and taking into account the boundary conditions yield,

$$v_\theta(0) = 0, \quad v_\theta(R) = R\omega,$$

and we obtain the following relation,

$$v_\theta = A_1 r + \frac{B_1}{r} = \omega r, \tag{16}$$

where $A_1 = \omega$ and $B_1 = 0$. When $r > R$, integrating (15) over r and taking into account the different boundary conditions yield,

$$v_\theta(+\infty) = 0, \quad v_\theta(R) = R\omega,$$

we have

$$v_\theta = A_2 r + \frac{B_2}{r} = \frac{\omega R^2}{r} \tag{17}$$

by considering the continuity condition at $r = R$, which leads $A_2 = 0$ and $B_2 = \omega R^2$.

Considering the balance of linear momentum in r-direction, we have

$$\rho\left(\frac{\partial v_r}{\partial t} + v_r\frac{\partial v_r}{\partial r} + \frac{v_\theta}{r}\frac{\partial v_r}{\partial \theta} + v_z\frac{\partial v_r}{\partial z} + \frac{v_\theta^2}{r}\right) = \frac{\partial \sigma_{rr}}{\partial r} + \frac{1}{r}\frac{\partial \sigma_{r\theta}}{\partial \theta} + \frac{\partial \sigma_{rz}}{\partial z} + \frac{2\sigma_{rr} - \sigma_{\theta\theta}}{r}. \tag{18}$$

In steady state, it can be simplified as

$$\frac{d\sigma_{rr}}{dr} + \frac{\sigma_{rr} - \sigma_{\theta\theta}}{r} = -\rho\frac{v_\theta^2}{r}, \tag{19}$$

with $\sigma_{rr} = \sigma_{\theta\theta} = -p_\omega, \rightarrow (\sigma_{rr} - \sigma_{\theta\theta})/r = 0$.

When $r < R$, substituting the stress term into the above equation, we can obtain,

$$-\frac{dp_\omega}{dr} = -\rho\frac{v_\theta^2}{r} = -\rho r\omega^2. \tag{20}$$

Integrating the above equation with respect to r, we can obtain,

$$p_\omega(r,\omega) = \frac{1}{2}\rho r^2\omega^2 + C_p \tag{21}$$

where r is the distance from the center of the centrifuge to the representative point that is under consideration, and the constant C_p is determined by the boundary pressure condition. Under this condition, $C_p = 0$.

Thus the centrifuge pressure on the surface of the membrane is,

$$f_\omega = p_\omega = \frac{1}{2}\rho r^2\omega^2, \quad r = R. \tag{22}$$

Considering the boundary pressure balance condition, we obtain the final expression for pressure difference near the pore location on the wall of the graphene centrifuge,

$$\Delta P = p_\omega - \Pi = \frac{1}{2}\rho R^2\omega^2 - \frac{C}{N_a}\frac{TN_i}{M_s}. \tag{23}$$

Considering the limit case $\Delta P = 0$, we obtain the expression for the critical angular velocity of the centrifuge,

$$\omega_{cr} = \frac{1}{R}\sqrt{\frac{2\Pi}{\rho}}, \tag{24}$$

which is the minimum or critical angular velocity required to starting the reverse osmosis desalination process.

To estimate the critical angular velocity, we may first examine the expression of critical angular velocity (24) for a few centrifuges of different radiuses. In Equation (24), if we choose $\Pi = 27.8$ bar $= 2.78$ *MPa*, $\rho = 0.99669 \times 10^3$ *kg/m*^{3}, we may find that: (a) When $R = 20.715$ *nm*, it leads to $\omega_{cr} = 3.5935$ *rad/ns*; (b) When $R = 1$ *m*, it leads to $\omega_{cr} = 74$ *rad/s* $= 706.65$ *rpm;* and (c) When $R = 10$ *m*, it leads to $\omega_{cr} = 7.4$ *rad/s* $= 70.665$ *rpm*. Obviously, for a scale-up porous centrifuge of radius 10 *m*, one can conduct an industrialized desalination operation by using the proposed centrifuge with an engineering attainable angular velocity.

The above relations are derived based on continuum scale fluid mechanics. However, since the size of nanoscale pores on the graphene wall have to be less than 1 nm for water molecule filtration, their applicability at nanoscale desalination is not automatically guaranteed. In the following, we carry out an alternative derivation of ΔP based on Molecular Dynamics, and the results based on two different approaches are compared in order to validate the fluid mechanics approach for future industrial scale nanoporous membrane centrifuge design. For an MD system of N atoms, the Hamiltonian is defined as:

$$\mathcal{H} = \frac{1}{2}\sum_{i=1}^{N} m_i v_i^2 + V_N \tag{25}$$

where m_i and v_i is the mass and velocity of the ith atom, V_N is the potential energy of the whole system.

When the molecular system is under rotation, it is better to examine it in the rotational coordinate frame. By assuming that a constant angular velocity ω along unit direction $\mathbf{e}_z$ is applied to the centrifuge, the atom velocity in the rotating frame ($\mathbf{v}'$) can be related to the velocity in fixed frame as follows,

$$\mathbf{v}_i = (\omega\,\mathbf{e}_z) \times \mathbf{r} + \mathbf{v}_i'. \tag{26}$$

Substituting the above equation into the Hamiltonian equation, we obtain

$$\mathcal{H} = \frac{1}{2}\sum_{i=1}^{N} m_i((\omega\,\mathbf{e}_z)\times\mathbf{r} + \mathbf{v}_i')_i^2 + V_N$$
$$= \frac{1}{2}\sum_{i=1}^{N} m_i(\mathbf{v}_i')^2 + \sum_{i=1}^{N} m_i\omega\,\mathbf{v}_i'\cdot(\mathbf{e}_z\times\mathbf{r}_i) + \frac{1}{2}\sum_{i=1}^{N} m_i\omega^2(\mathbf{e}_z\times\mathbf{r}_i)^2 + V_N.$$

Let $\mathbf{q}_i = \mathbf{r}_i$ and $\mathbf{p}_i = m_i\,\mathbf{v}_i'$. Hamiltonian equations of motion read as,

$$\frac{d\mathbf{p}_i}{dt} = \mathbf{F}_i' = -\frac{\partial\mathcal{H}}{\partial\mathbf{r}_i}$$
$$= -\omega\,\mathbf{p}_i\cdot\frac{\partial}{\partial\mathbf{r}_i}(\mathbf{e}_z\times\mathbf{r}_i) - \omega^2 m_i(\mathbf{e}_z\times\mathbf{r}_i)\cdot\frac{\partial}{\partial\mathbf{r}_i}(\mathbf{e}_z\times\mathbf{r}_i) - \frac{\partial V_N}{\partial\mathbf{r}_i}.$$

Defining $\mathbf{F} = -\frac{\partial V_N}{\partial\mathbf{r}_i}$, which is the force in the fixed frame. Converting the above equation in Cartesian components, we have

$$F_{ix}' = F_{ix} + \omega\,m_i v_{iy}' + \omega^2 m_i r_{ix}$$
$$F_{iy}' = F_{iy} - \omega\,m_i v_{ix}' + \omega^2 m_i r_{iy}\,.$$
$$F_{iz}' = F_{iz}$$

From the above equations, we can see that the force component in the *z*-direction does not change, but the force components in the *x* and *y* directions changed, and they coupled together through velocity terms. The difference $\mathbf{F}^i_{rel} = \mathbf{F}_i - \mathbf{F}_i$ is the relative force of water molecule i applied on the graphene wall, if the centrifuge is rotating along *z*-axis, i.e. $\omega\mathbf{e}_z$. To calculate the pressure on the graphene wall, we can calculate the radial and tangential force components by using the following transform,

$$F_{rel}^{ir} = F_{rel}^{ir}\,cos(\theta) + F_{rel}^{iy}\,sin(\theta) = \frac{1}{r_i}\left(r_{ix}F_{rel}^{ir} + r_{iy}F_{rel}^{iy}\right)$$
$$= \frac{\omega\,m_i}{r_i}\left(r_{ix}v_{iy}' - r_{iy}v_{ix}'\right) + \omega^2 m_i r_i \qquad (27)$$

$$F_{rel}^{i\theta} = -F_{rel}^{ix}\,sin(\theta) + F_{rel}^{iy}\,cos(\theta) = \frac{1}{r_i}\left(-r_{iy}F_{rel}^{ix} + r_{ix}F_{rel}^{iy}\right)$$
$$= -\frac{\omega\,m_i}{r_i}\left(r_{ix}v_{ix}' + r_{iy}v_{iy}'\right) \qquad (28)$$

where $r_i = \sqrt{r_{ix}^2 + r_{iy}^2}$. The term $F_{rel}^{i\theta}$ is the Coriolis force, which may push the ion particles moving tangentially relative to the rotating centrifuge and provides a self-assisted or intrinsic anti-fouling ability; and F_{rel}^{ir} is the centrifugal force, which may be converted to "centrifugal pressure" by using the following expression,

$$p_\omega = \frac{\sum_{i=1}^{N_{H_2O}} F_{rel}^{ir}}{A_{cnt}} \qquad (29)$$

where A_{cnt} is the total area of the graphene wall, N_{H_2O} is the total number of water molecules within a distance of 1 *nm* to the graphene wall.

5. MATERIALS AND METHODS

Figure 9 shows a snapshot sequence of a MD simulation process in nanoscale, a molecular scale reverse-osmosis desalination process conducted by a virtual nanoporous membrane centrifuge, and thus it demonstrates the proof of concept.

For the proposed graphene centrifuge model, the size of the centrifuge can go from nanoscale to macroscale. Since it will be difficult to use MD to simulate a macroscale centrifuge, we shall build a nano-size structure and mainly reply on the prediction of fluid mechanics analysis. A CNT served as graphene membrane cylinder with chirality number (400,200) and length 10 *nm* is built, and 20 pores are created on the graphene wall with pore radius $r_p = 0.284$ *nm* as shown in **Fig. 10**.

The above model is solvated into a water box with dimension of 45 × 45 × 10.14 *nm*, in which there area total of 1,306,595 water molecules that are modeled by using SPC/E model[21]. Na^+ and Cl^- ions are added inside the cylinder with a total number of 9866 pairs, which corresponds to the concentration of salt ions in seawater (35 g/L). From the above parameters, we can obtain the diameter, surface area and volume of the giant CNT,

$$D_{cnt} = \frac{0.246}{\pi}\times\sqrt{400^2 + 400\times200 + 200^2} = 41.43\ nm$$
$$A_{cnt} = \pi\times D_{cnt}\times10 = 1301.7\ nm^2$$
$$V_{cnt} = \frac{\pi}{4}D_{cnt}^2\times10 = 13480.93\ mn^3$$

The open source molecular dynamics software package, Gromacs[18], is used in the calculation. The OPLS force field[22] is selected to describe the bond strength between different atoms and molecules. A total simulation time of 3 *ns* was conducted with data in the last 2 *ns* is used for data analysis. The integration time step is chosen as 1 *fs*, and the data are collected every 0.5 *ps*.

The MD simulation is performed in three steps: We first start with an NVT calculation by using the Nose-Hoover thermostat[23] to maintain a temperature at 298 *K*, and then the MD simulation is run as an NPT ensemble. The size of the simulation box depends on the dimensions of the centrifuge, and periodic boundary conditions in all directions are employed. The particle mesh Ewald method[24] is used for calculating electrostatic interactions, and the cut-off of the Lennard-Jones (LJ) interactions is set at 0.6 *nm* in all three directions. The neighbor list is updated at every step to avoid intrinsic errors[25].

The porous CNT system is subjected to a prescribed angular velocity ranging from 0.1 *rad/ns* to 60 *rad/ns* in the simulation. The CNT may be assumed to be stationary in a rotating frame, and the rotational motions of water molecules, Na^+ and Cl^- ions, are generated by the inter-molecular interaction between the CNT with water molecules and with ions, and the complex interactions among themselves.

To calculate the energy efficiency, we also build a relatively smaller model with chirality number (200,100), and a calculation with longer simulation time of 30 *ns* was conducted. The numerical model contains a total of 317,965 water molecules. Similar conditions for the MD calculation was set for this model. The efficiency result is depicted in **Fig. 7**. It is seen that the efficiency of the centrifuge has been increasing up to 30 ns. Hence, we think that the given efficiency result is reasonable.

On the other hand, we can compare the prediction of fluid mechanics with the molecular dynamics simulation results in the nanoscale to correlate the two different approaches. It is noted that in the fluid mechanics approach, the rotation motion of the liquid is caused by the rotation of the graphene wall. The fluid motion inside the centrifuge is solved as a standard boundary value problem of the Taylor-Couette flow problem, e.g. Ref. 26. The same can be said in the MD simulation, in which the rotating motion of the graphene centrifuge is prescribed, while the motions of water molecules and ions are calculated based on the molecular dynamics equations of motions.

In passing, we note that once the angular velocity of the centrifuge exceeds a certain value, hydrodynamics instability and turbulence flow will occur. This type of instability can also be observed in the MD simulation, which may affect the efficiency of the desalination process. To focus

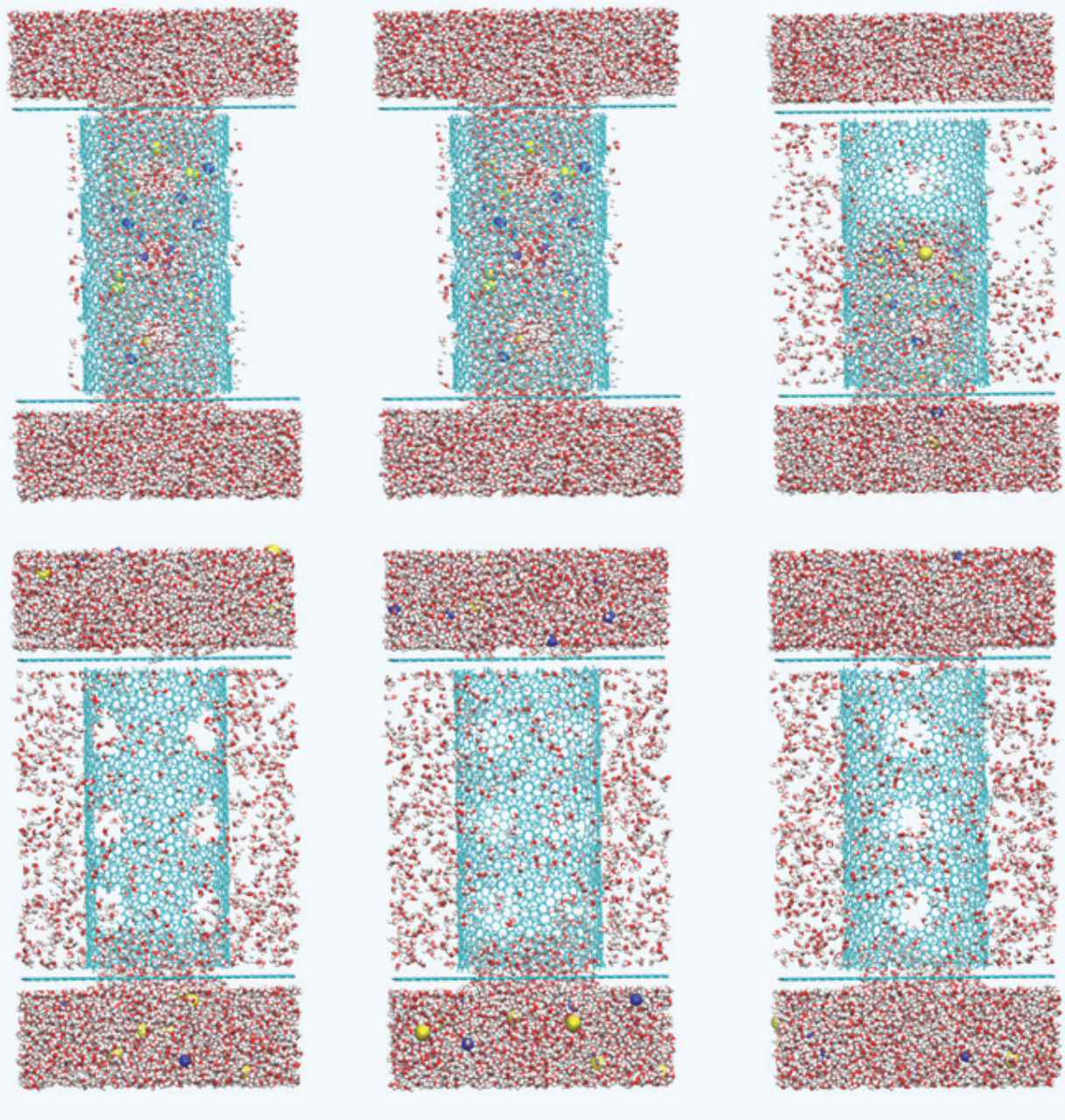

Figure 9 The proof of concept: A molecular reverse-osmosis desalination process conducted by the nanoporous membrane centrifuge.

on the main task at hand, this aspect of the phenomenon will be reported in a separate paper, based on its own scientific merits.

The porosity of the model is calculated as $\varepsilon = 0.00389$. The permeability of the model, the water flux, and volumetric flow rate are computed, and listed as follows,

$$A = \frac{\varepsilon r_p^2}{8\mu_0 L_m} = 23.285\ (LMH/bar)$$
$$J_w = A\Delta P = 0.065\Delta P \times 10^{-4}\ (m/s) = 23.285\Delta \mathrm{P}\ (LMH)$$
$$Q = J_w A_{cnt} = 8.46\Delta P \times 10^{-21}\ m^3/s = 0.28\Delta P\ (H_2O/ns)$$

In the above calculation, it is assumed that the density of solute is $\rho = 10^3\ kg/m^3$, and molar mass is $M_{H_2O} = 18.01528\ g/mol$. The mass of water molecules inside graphene membrane centrifuge is calculated as: $M_s = \rho V_{cnt} = 1.348 \times 10^{-20}\ kg$. It may be noted that the porosity of the model is calculated for the case of total 20 holes on the graphene membrane wall with the radius of 0.284 *nm*. Obviously, if we increase the number of holes, the porosity of the number may increase significantly, and so will the permeability of the model. Finally, we obtain the osmosis pressure and the centrifugal pressure ($R = 20.715\ nm$),

$$\Pi = \frac{C}{N_a}\frac{TN_i}{M_s} = 7.61N_i = 27.8\ (Bar)$$
$$p_\omega = \frac{1}{8}\rho D_{cnt}^2\omega^2 = 2.15\omega^2\ (Bar)$$

where the angular velocity ω has the unit of *rad*/*ns*.

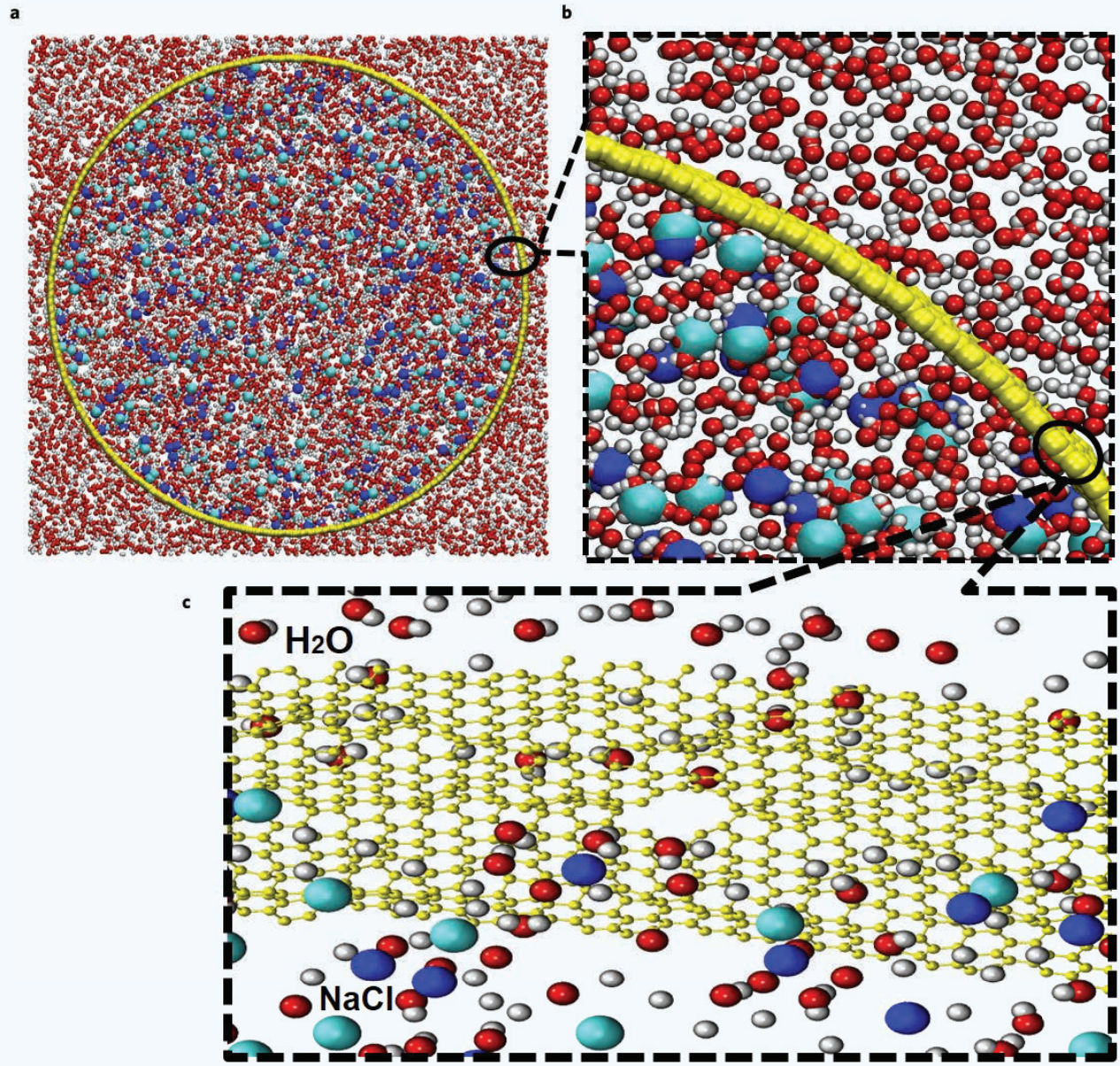

Figure 10 Water molecule distribution inside and outside the pore on the wall of the centrifuge (at $t = 4$ *ns*): (**a**) Section view of centrifuge; (**b**) zoom-in view, and (**c**) three-dimensional zoom-in view.

The analytical expressions of pressure difference ΔP (N_i, ω) and volumetric flow rate Q (N_p, r_p, D_{cnt}, N_i, ω) as a function of only ω will be compared with numerical results conducted by MD simulation; their corresponding final expressions are summarized here (with other parameters fixed):

$$\Delta P = 2.15\omega^2 - 27.8 \ (Bar) \tag{30}$$

$$Q = 0.28\Delta P = 0.602\omega^2 - 7.78 \ (H_2O/ns) \tag{31}$$

Based on the above parameters, we find the minimum angular velocity required to counter-balance the osmotic pressure for a 20.715 *nm* radius centrifuge is $\omega_{cr} = 3.6$ *rad/ns*.

CONFLICTS OF INTEREST

The author declares no conflict of interest.

ABBREVIATIONS

The following abbreviations are used in this manuscript:

MD	Molecular Dynamics
CNT	Carbon Nanotube
OPLS	Optimized Potentials for Liquid Simulations
NVT	Molecular dynamics ensemble with constant: Number of atoms (N), Volume (V) and Temperature (T)
NPT	Molecular dynamics ensemble with constant: Number of atoms (N), Pressure (P) and Temperature (T)
SPC/E	Extended Simple Point Charge

REFERENCES

1. Hummer, G., Rasaiah, J.C. & Noworyta, J.P. Water conduction through the hydrophobic channel of a carbon nanotube. *Nature* **414**(6860), 188–190 (2001).
2. Kalra, A., Garde, S. & Hummer, G. Osmotic water transport through carbon nanotube membranes. *Proc. Natl. Acad. Sci. U.S.A.* **100**(18), 10175–10180 (2003).
3. Holt, J.K., Park, H.G., Wang, Y., Stadermann, M., Artyukhin, A.B., Grigoropoulos, C.P., Noy, A. & Bakajin, P. Fast mass transport through sub-2-nanometer carbon nanotubes. *Science* **312**(5776), 1034–1037 (2006).
4. Fornasiero, F., Park, H.G., Holt, J.K., Stadermann, M., Grigoropoulos, C.P., Noy, A. & Bakajin, O. Ion exclusion by sub-2-nm carbon nanotube pores. *Proc. Natl. Acad. Sci. U.S.A.* **105**(45), 17250–17255 (2008).
5. Corry, B. Designing carbon nanotube membranes for efficient water desalination. *J. Phys. Chem. B* **112**(5), 1427–1434 (2008).
6. Corry, B. Water and ion transport through functionalised carbon nanotubes: Implications for desalination technology. *Energy Environ. Sci.* **4**(3), 751–759 (2011).
7. Humplik, T., Lee, J., Ohern, S.C., Fellman, B.A., Baig, M.A., Hassan, S.F., Atieh, M.A., Rahman, F., Laoui, T., Karnik, R. & Wang, E.N. Nanostructured materials for water desalination. *Nanotechnology* **22**(29), 292001 (2011).
8. Das, R., Ali, M.E., Hamid, S.B.A., Ramakrishna, S. & Chowdhury, Z.Z. Carbon nanotube membranes for water purification: A bright future in water desalination. *Desalination* **336**, 97–109 (2014).
9. Liu, J., Shi, G., Yang, J. & Fang, H. Blockage of water flow in carbon nanotubes by ions due to interactions between cations and aromatic rings. *Phys. Rev. Lett.* **115**, 164502 (2015).
10. Fan, X., Liu, Y., Quan, X., Zhao, H., Chen, S., Yi, G. & Du, L. High desalination permeability, wetting and fouling resistance on superhydrophobic carbon nanotube hollow fiber membrane under self-powered electrochemical assistance. *J. Membr. Sci.* **514**, 501–509 (2016).
11. Cohen-Tanugi, D. & Grossman, J.C. Water desalination across nanoporous graphene. *Nano Lett.* **17**(7), 3602–3608 (2012).
12. Kar, S., Bindal, R.C. & Tewari, P.K. Carbon nanotube membranes for desalination and water purification: Challenges and opportunities. *Nano Today* **7**(5), 385–389 (2012).
13. Tu, Q., Yang, Q., Wang, H. & Li, S. Rotating carbon nanotube membrane filter for water desalination. *Sci. Rep.* **66**, 26183 (2016).
14. Zhu, X., Villeneuve, D.M., Naumov, A.Y., Nikumb, S. & Corkum, P.B. Experimental study of drilling sub-10m holes in thin metal foils with femtosecond laser pulses. *Appl. Surf. Sci.* **152**(3), 138–148 (1999).
15. O'Hern, S.C., Boutilier, M.S.H., Idrobo, J.C., Song, Y., Kong, J., Laoui, T., Atieh, M. & Karnik, R. Selective ionic transport through tunable subnanometer pores in single-layer graphene membranes. *Nano Lett.* **14**(3), 1234–1241 (2014).
16. Fischbein, M.D. & Drndić, M. Electron beam nanosculpting of suspended graphene sheets. *Appl. Phys. Lett.* **93**(11), 113107 (2008).
17. Mancinelli, R., Botti, A., Bruni, F., Ricci, M.A. & Soper, A.K. Hydration of sodium, potassium, and chloride ions in solution and the concept of structure maker/breaker. *J. Phys. Chem. B* **111**(48), 13570–13577 (2007).
18. van der Spoel, D., Lindahl, E., Hess, B., Groenhof, G., Mark, A.E. & Berendsen, H.J.C. GROMACS: Fast, flexible, and free. *J. Comput. Chem.* **26(**16), 1701–1718 (2005).
19. Li, T., Tu, Q. & Li, S. Molecular dynamics modeling of nano-porous centrifuge for reverse osmosis desalination. *Desalination*, in press, https://doi.org/10.1016/j.desal.2017.09.015 (2017).
20. Scatchard, G. Physical chemistry of protein solutions. I. Derivation of the equations for the osmotic pressure. *J. Am. Chem. Soc.* **68**(11), 2315–2319 (1946).
21. Berendsen, H.J.C., Grigera, J.R. & Straatsma, T.P. The missing term in effective pair potentials. *J. Phys. Chem.* **91**(24), 6269–6271 (1987).
22. Jorgensen, W.L. & Tirado-Rives, J. The OPLS optimized potentials for liquid simulation potential functions for proteins, energy minimizations for crystals of cyclic peptides and crambin. *J. Am. Chem. Soc.* **110**(6), 1657–1666 (1988).
23. Nosé, S. A unified formulation of the constant temperature molecular dynamics methods. *J. Chem. Phys.* **81**(1), 511–519 (1984).
24. Essmann, U., Perera, L., Berkowitz, M.L., Dardenand, T., Lee, H. & Pedersen, L.G. A smooth particle mesh Ewald method. *J. Chem. Phys.* **103**(19), 8577–8593 (1995).
25. Cino, E.A., Wong-Ekkabut, J., Karttunen, M. & Choy, W.-Y. Microsecond molecular dynamics simulations of intrinsically disordered proteins involved in the oxidative stress response. *PLoS One* **6**(11), e27371 (2011).
26. Andereck, C.D., Liu, S.S. & Swinney, H.L. Flow regimes in a circular Couette system with independently rotating cylinders. *J. Fluid Mech.* **164**, 155–183 (1986).